DTU Library

Optomagnetic detection of DNA triplex nanoswitches

Minero, Gabriel Khose Antonio; Fock, Jeppe; McCaskill, John S; Hansen, Mikkel Fougt

Optomagnetic detection of DNA triplex nanoswitches†

Gabriel Antonio S. Minero,[a,b] Jeppe Fock,[a] John S. McCaskill,[b] and Mikkel F. Hansen[a†]

We report on optomagnetic dose-dependent detection of DNA triplex-mediated and pH-switchable clusters of functionalised magnetic nanoparticles.

Polypurine-polypyrimidine sequences can fold into triple helical DNA structures forming T-A-T and C-G-C$^+$ nucleobase triplets upon protonation of cytosine bases at pH $\leq$ 6.[1] The predictable and pH-controlled base pairing makes triplex-forming sequences very useful for programming chemical reactions,[2,3] nanomachines,[4,5] nanostructures,[6–8] and hydro-gels.[9,10] Switching of pH-responsive DNA composites can be employed for controlled release of targets in delivery systems[11,12] and in on/off regulation of the nanoscale devices upon cyclic alternation of pH values.[13]

Further, triplex-forming sequences of DNA are known to play a significant role in genetic regulation.[14–17] Conditions favouring triplex binding can be screened using fluorescent molecular probes[18,19] or by DNA mobility shift assays.[17] For the latter, the assay time can be reduced to 10-15 min using capillary gel electrophoresis.[3,9] Palindromic homopurine-homopyrimidine tracts have been shown to cause a pH-dependent structural transition of a plasmid DNA *in vivo* and have been observed during the initial replication of tumor viruses.[20] Therefore, dose-dependent detection of polypurine tracts (PPT) in human and viral genomes can contribute to molecular diagnostics of genetic biomarkers such as the conserved PPT region of HIV-1.[21]

Label-free detection of DNA targets has been demonstrated with high selectivity and sensitivities in the 0.05 - 10 nM range using electrochemical biosensors.[22] Multi-step DNA processing has further decreased sensitivities to the sub-pM range.[23,24] Electrochemical detection of triplex DNA formation of double-stranded DNA targets with DNA probes on an electrode surface has been demonstrated directly in complex sample matrices, such as blood serum, with a limit of detection (LOD) of about 10 nM.[21] Analysis of triplex formation of a PPT target as short as 10 bases was demonstrated down to nM concentrations.[25]

Nanoscale optical DNA sensing was examined using confocal microscopy of light-emitting nanowires functionalised with p-DNA resulting in an LOD of 100 aM.[26] Colorimetric detection of DNA based on agglutination of gold nanoparticle (NP) was reported for target DNA concentrations of 75 nM,[27] 150 nM,[28] and 3.3 µM.[29] The LOD could be reduced to 0.1 pM via dark field microscopy imaging.[27] The duplex DNA-induced NP aggregation required 2 h of incubation. For triplex DNA hybridisation prolonged incubation times of 12 h and 24 h were needed.[29,30]

Magnetic nanoparticles (MNPs) are increasingly being used for robust solid phase analyte detection,[31–33] and for delivery of small molecules.[34–36] Recently, an optomagnetic method to detect agglutination of MNPs was proposed and used to detect DNA from different pathogenic bacteria after rolling circle amplification[33] as well as to investigate the Cu^{2+} binding properties of metformin.[32] The method measures the modulation of laser light transmitted through the sample container in response to an applied oscillating magnetic field. This modulation arises from the coupled magnetic and optical anisotropies of the MNPs and is highly sensitive to size-changes of the MNPs due to agglutination.[33]

Here, we employ the optomagnetic readout principle (Fig. 1A) to investigate reversible triplex DNA formation (Fig. 1B). A single population of MNPs is functionalised with palindromic polypyrimidine DNA oligonucleotides. At pH $\leq$ 6, a triplex structure will form between two palindromic polypyrimidine DNA strands situated on separate MNPs and a polypurine target DNA in suspension. Thus, the presence of the target DNA

causes formation of MNP clusters at pH ≤ 6. The kinetics of cluster formation is accelerated by application of a strong magnetic field (magnetic incubation). We show that the magnetic incubation combined with the optomagnetic readout reduces the assay time to a few minutes (Section S3†).

Two previously presented setups were used: the first setup was adapted for a cuvette[37] (Fig. 1A), where pH titration was easy to handle; the second setup included a fully automated lab-on-a-disc sample handling including sequential magnetic incubation and readout of up to 18 sample pools.[33] In brief, a sinusoidally varying external magnetic field modulates the transmission of monochromatic light (λ = 405 nm) as the MNPs cyclically relax away from and align towards the magnetic field direction. The real and imaginary components V_2' and V_2'' of the 2$^{\text{nd}}$ harmonic signal are normalised with the average signal, V_0, to account for variations in the incoming light intensity. More information about the optomagnetic method can be found in Section S1†. Experiments involving switching of triplex DNA were carried out in the cuvette setup.
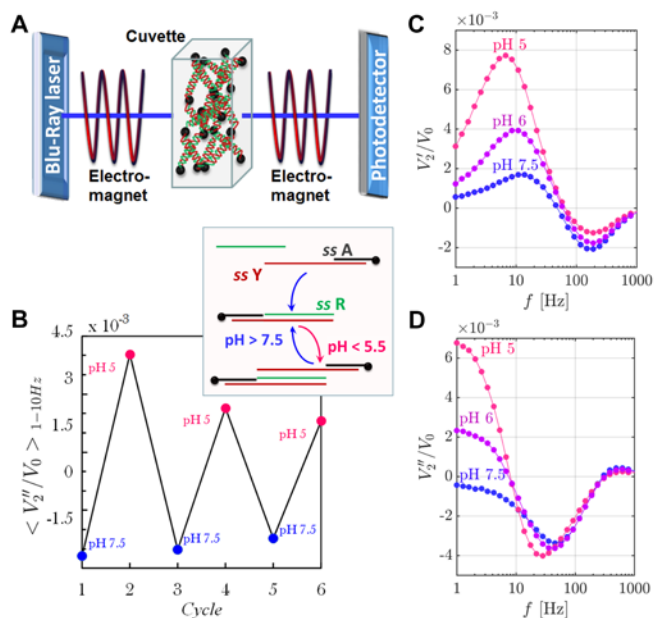

Fig. 1: pH-dependent optomagnetic detection of triplex DNA nanoswitches. (A) Setup for optomagnetic monitoring of MNP agglutination.[37] (B) Optomagnetic detection of pH nanoswitches; DNA sequences are listed in Table S1†. (C-D). Triplex DNA processing at pH 7.5, 6.0, and 5.0 for 0.2 mg/ml MNPs (at intermediate probe density, 50 p-DNA per MNP) in

the presence of 1 nM target ss DNA. (C) V_2'/V_0 and (D) V_2''/V_0 vs frequency. Magnetic incubation of the mixed samples for 2 min in 20 mT magnetic field was used to accelerate DNA-mediated agglutination. More information about the probe density is given in Fig. S1†.

As a proof of principle, we first measured the pH dependence of the system response at three pH values (Fig. 1C-D). The obtained optomagnetic spectra can be divided into two regions; one above 50 Hz and one below 50 Hz. In V_2'/V_0 (Fig. 1C), the negative peak above 50 Hz corresponds to free MNPs.[37,38] Below 50 Hz, a positive peak in V_2'/V_0 is observed, which arises from clusters with a circumference larger than the wavelength. The sign change is due to a change in the scattering properties of the larger particles.[37] In V_2''/V_0 (Fig. 1D), the signal below 50 Hz is composed of a negative contribution to the signal from free MNPs and positive contributions from MNP clusters.

For pH decreasing from 7.5 to 5.0, we observed a decrease in the negative V_2'/V_0 peak at about 200 Hz in Fig. 1C (depletion of free MNPs) and, correspondingly, an increase in the positive signal at $f < 50$ Hz (formation of clusters). Both effects contribute to an increasing signal in V_2''/V_0 below 10 Hz in Fig 1D. Without magnetic incubation, however, the spectra were almost identical to that of the no-target sample (Fig. S2†). For further analysis, we used the average signal $\langle V_2''/V_0 \rangle_{1-10\,\text{Hz}}$ at f = 1-10 Hz, as this provided the largest response to the cluster formation. The obtained pH-dependence of the optomagnetic signal was consistent with our studies of the triplex switching reported previously.[3] The nanoswitches between stable (pH < 5.5) and unstable (pH > 7.5) conditions for triplex formation were observed to behave reversibly and to be clearly detectable in the optomagnetic signal (Fig. 1B). We also investigated real-time detection of melting DNA bridges between MNPs and the resulting depletion of MNP clusters at low pH (Fig. S3†). The obtained trends of optomagnetic signal vs. temperature were consistent with melting of the triplex DNA (broad melting transition at 45-55°C).[3]

Below, all optomagnetic signals were measured after automated magnetic incubation on a disc.[33] The presence of matching DNA target (0.1-2 nM) revealed clustering of MNPs via formation of triplex DNA **Y•R•Y** at conditions favourable for triplex formation (pH 5.0) (Fig. 2A). These were seen in the low-frequency response as discussed in the previous section and in Section S5†. The specificity of the triplex formation was investigated using a non-matching DNA for which no detectable changes in V_2'' were observed (Fig. S4†).
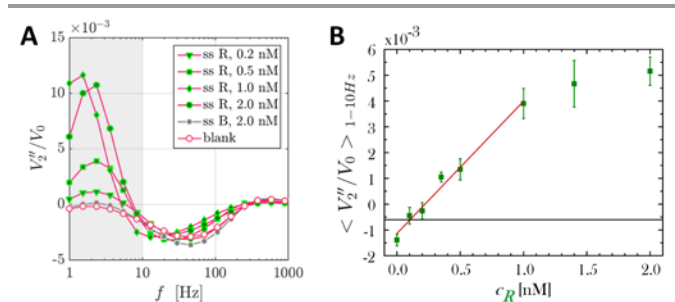

Fig. 2: Dose-dependent analysis of optomagnetic signal from the MNPs/p-DNA in the presence of matching target DNA. (A) Optomagnetic spectra from the sequence specific **Y•R•Y** at pH 5.0. (B) $\langle V_2''/V_0 \rangle_{1-10\,\text{Hz}}$ vs. concentration of polypurine target DNA. The black line represents the LOD obtained as the signal from the no-target sample plus three times its standard deviation. See Section S2† for more details on the assay.

It is well known that the gain of DNA sensors is a complex function of the capture probe packing density.[22,39] For the MNP concentration of 0.2 mg/ml, we observed the most sensitive detection of target at intermediate packing density (50 p-DNA probes per MNP), see Fig. S5†.

Electrochemical biosensors have been applied for label-free detection of DNA targets at sub-pM concentrations, but they require several fabrication steps (4-5 steps[22,23] taking more than 24 h), external stimuli for amplification of the signal, e.g., via conformational changes of DNA probes on the electrode surface and are also sensitive to the liquid properties. The presented MNP-based readout has the advantages that a sensitive detection scheme can be applied for any liquid suspension of the MNPs and that the magnetic incubation reduces the assay time to a few minutes compared to for example 12 h, which has been reported for the assembly of gold nanoparticles.[30]

In conclusion, we have demonstrated optomagnetic detection of 0.1-2 nM polypurine target DNA via triplex folding in the presence of magnetic nanoparticles with complementary palindromic DNA probes attached to the surface. The strong signal at low frequencies solely observed in the presence of the matching target and for pH 5, indicates agglutination of the MNPs via triplex formation. The obtained MNP clusters can be switched by pH, with a reaction time reduced to less than 10 min using magnetic incubation. Although our approach is limited to homopurine or homopyrimidine triplex-forming sequences, it can be extended to non-palindromic target and probes by introducing a second population of functionalised MNPs according to **Y₁•R•Y₂**. Targets can be identified as polypurine sub-sequences of 16-20 bases, which are commonly found in human and pathogen genomes.[25] Moreover, the recognition length of PPTs can even be reduced to 10 nt by introducing synthetic modifications in the probes.[40] With this in mind, the approach can be extended to be compatible with physiological conditions (pH ~ 7).[41]

Notes and references

1   G. E. Plum, D. S. Pilch, S. F. Singleton and K. J. Breslauer, *Annu. Rev. Biophys. Biomol. Struct.*, 1995, **24**, 319–350.

2   Y. Chen and C. Mao, *J. Am. Chem. Soc.*, 2004, **126**, 13240–13241.

3   G. A. S. Minero, P. F. Wagler, A. a. Oughli and J. S. McCaskill, *RSC Adv.*, 2015, **5**, 27313–27325.

4   D. Liu and S. Balasubramanian, *Angew. Chemie - Int. Ed.*, 2003, **42**, 5734–5736.

5   Y. Chen, S. H. Lee and C. Mao, *Angew. Chemie - Int. Ed.*, 2004, **43**, 5335–5338.

6   Y. Kawabata, T. Ooya, W. K. Lee and N. Yui, *Macromol. Biosci.*, 2002, **2**, 195–198.

7   Y. Chen, H. Liu, T. Ye, J. Kim and C. Mao, *J. Am. Chem. Soc.*, 2007, **129**, 8696–8697.

8   D. A. Rusling, I. S. Nandhakumar, T. Brown and K. R. Fox, *ACS Nano*, 2012, **6**, 3604–3613.

9   P. Wagler, G. A. S. Minero, U. Tangen, J. W. De Vries, D. Prusty, M. Kwak, A. Herrmann and J. S. Mccaskill, *Electrophoresis*, 2015, **35**, 2451.

10   W. Guo, C. Lu, R. Orbach, F. Wang, X. Qi, A. Cecconello, D. Seliktar and I. Willner, *Adv. Mater.*, 2015, 73–78.

11   C. Sun, J. S. H. Lee and M. Zhang, *Adv. Drug Deliv. Rev.*, 2008, 60, 1252–1265.

12   V. V. Mody, A. Cox, S. Shah, A. Singh, W. Bevins and H. Parihar, *Appl. Nanosci.*, 2013, **4**, 385–392.

13   K. Haruna, H. Iida, K. Tanabe and S. Nishimoto, *Org. Biomol. Chem.*, 2008, **6**, 1613–1617.

14   N. Baran, A. Lapidot and H. Manor, *Proc. Natl. Acad. Sci. U. S. A.*, 1991, **88**, 507–511.

15   A. Dayn, G. M. Samadashwily and S. M. Mirkin, *Proc. Natl. Acad. Sci. U. S. A.*, 1992, **89**, 11406–11410.

16   G. M. Samadashwily, A. Dayn and S. M. Mirkin, *EMBO J.*, 1993, **12**, 4975–4983.

17   L. D. Nelson, C. Bender, H. Mannsperger, D. Buergy, P. Kambakamba, G. Mudduluru, U. Korf, D. Hughes, M. W. Van Dyke and H. Allgayer, *Mol. Cancer*, 2012, **11**, 38.

18   K.-C. Lin, C.-Y. Kuo, C.-C. Nieh and W.-L. Tseng, *RSC Adv.*, 2014, **4**, 38389–38392.

19   A. Idili, A. Vallée-Bélisle and F. Ricci, *J. Am. Chem. Soc.*, 2014, **136**, 5836–5839.

20   V. Kopel, A. Pozner, N. Baran and H. Manor, *Nucleic Acids Res.*, 1996, **24**, 330–335.

21   A. Patterson, F. Caprio, A. Vallee-Belisle, D. Moscone, K. W. Plaxco, G. Palleschi and F. Ricci, *Anal. Chem.*, 2010, **82**, 9109–9115.

22   X. Wang, A. Jiang, T. Hou and F. Li, *Anal. Chim. Acta*, 2015, **890**, 91–97.

23   M. Xu, J. Zhuang, X. Chen, G. Chen and D. Tang, *Chem. Commun. (Camb).*, 2013, **49**, 7304–6.

24   Q. Wang, F. Gao, J. Ni, X. Liao, X. Zhang and Z. Lin, *Sci. Rep.*, 2016, **6**, 22441.

25   A. Idili, A. Amodio, M. Vidonis, J. Feinberg-Somerson, M. Castronovo and F. Ricci, *Anal. Chem.*, 2014, **86**, 9013–9019.

26   D. H. Park, N. Kim, C. Cui, Y. K. Hong, M. S. Kim, D.-H. Yang, D.-C. Kim, H. Lee, J. Kim, D. J. Ahn and J. Joo, *Chem. Commun. (Camb).*, 2011, **47**, 7944–6.

27   T. Bu, T. Zako, M. Fujita and M. Maeda, *Chem. Commun. (Camb).*, 2013, **49**, 7531–3.

28   M. S. Han, A. K. R. Lytton-Jean and C. A. Mirkin, *J. Am. Chem. Soc.*, 2006, **128**, 4954–4955.

29   X. Zhu, Y. Liu, J. Yang, Z. Liang and G. Li, *Biosens. Bioelectron.*, 2010, **25**, 2135–2139.

30   H. Yan, C. Xiong, H. Yuan, Z. Zeng and L. Ling, *J. Phys. Chem. C*, 2009, **113**, 17326–17331.

31   H. Yin, H. Kuang, L. Liu, L. Xu, W. Ma, L. Wang and C. Xu, *ACS Appl. Mater. Interfaces*, 2014, **6**, 4752–4757.

32   X. Quan, R. Uddin, A. Heiskanen, M. Parmvi, K. Nilson, M. Donolato, M. F. Hansen, G. Rena and A. Boisen, *Chem. Commun.*, 2015, **51**, 17313–17316.

33   A. Mezger, J. Fock, P. Antunes, F. W. Østerberg, A. Boisen, M. Nilsson, M. F. Hansen, A. Ahlford and M. Donolato, *ACS Nano*, 2015, **9**, 7374–7382.

34   T. M. Allen and P. R. Cullis, *Science*, 2004, **303**, 1818–1822.

35   Y. H. Jung, K. B. Lee, Y. G. Kim and I. S. Choi, *Angew. Chemie - Int. Ed.*, 2006, **45**, 5960–5963.

36   C. Zhao, K. Qu, J. Ren and X. Qu, *Chemistry*, 2011, 1–8.

37   M. Donolato, P. Antunes, R. S. Bejhed, T. Zardán Gómez de la Torre, F. W. Østerberg, M. Strömberg, M. Nilsson, M. Strømme, P. Svedlindh, M. F. Hansen and P. Vavassori, *Anal. Chem.*, 2015, **87**, 1622–1629.

38   J. Fock, M. Parmvi, M. Strömberg, P. Svedlindh, M. Donolato and M. F. Hansen, *Biosens. Bioelectron.*, 2017, **88**, 94-100.

39   K. B. Cederquist and C. D. Keating, *Langmuir*, 2010, **26**, 18273–18280.

40   K. R. Fox and T. Brown, *Biochem. Soc. Trans.*, 2011, **39**, 629–634.

41   D. A. Rusling, L. Le Strat, V. E. C. Powers, V. J. Broughton-Head, J. Booth, O. Lack, T. Brown and K. R. Fox, *FEBS Lett.*, 2005, **579**, 6616–6620.